

Lab on a Chip

Accepted Manuscript



This is an *Accepted Manuscript*, which has been through the Royal Society of Chemistry peer review process and has been accepted for publication.

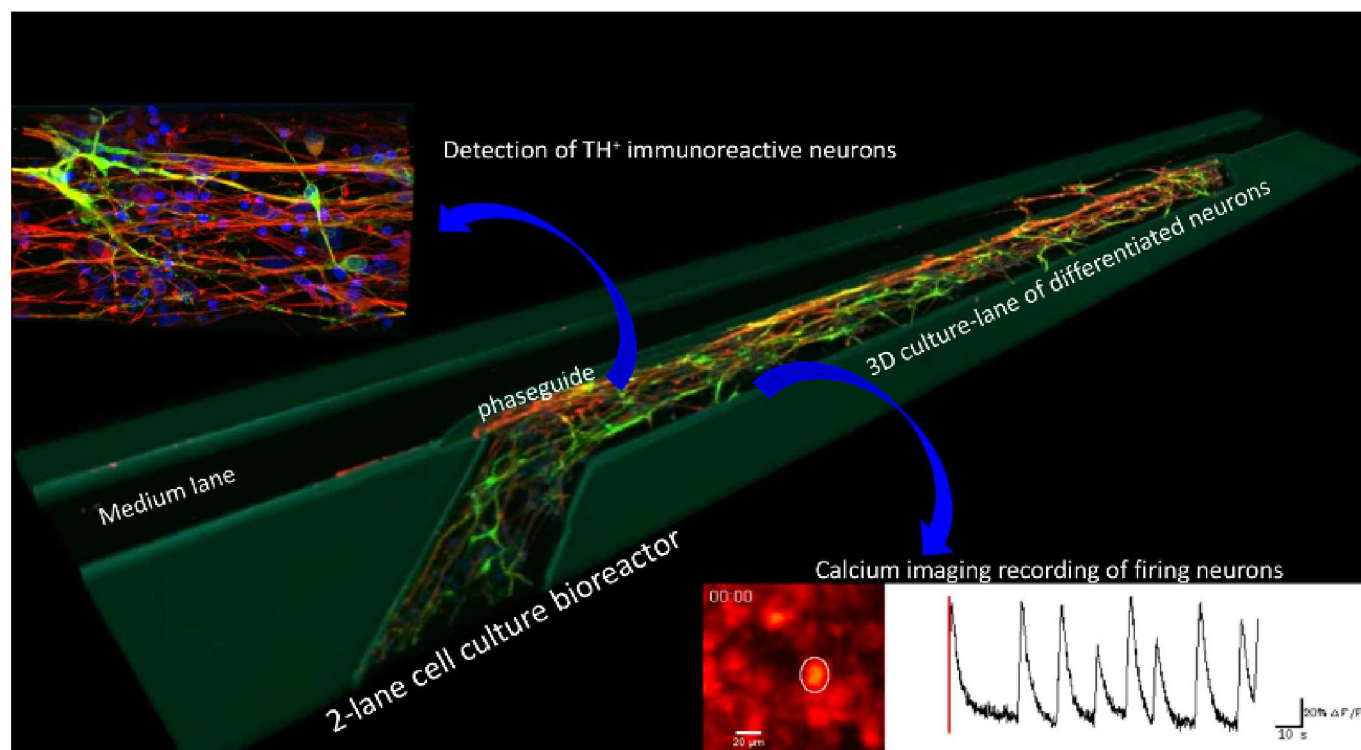
Accepted Manuscripts are published online shortly after acceptance, before technical editing, formatting and proof reading. Using this free service, authors can make their results available to the community, in citable form, before we publish the edited article. We will replace this *Accepted Manuscript* with the edited and formatted *Advance Article* as soon as it is available.

You can find more information about *Accepted Manuscripts* in the [Information for Authors](#).

Please note that technical editing may introduce minor changes to the text and/or graphics, which may alter content. The journal's standard [Terms & Conditions](#) and the [Ethical guidelines](#) still apply. In no event shall the Royal Society of Chemistry be held responsible for any errors or omissions in this *Accepted Manuscript* or any consequences arising from the use of any information it contains.

Table of Contents Entry

Colour Graphic



Text

Efficient differentiation of hNESCs into mature and functional dopaminergic neurons in phase-guided 3D microfluidic cell cultures.

Differentiation of neuroepithelial stem cells into functional dopaminergic neurons in 3D microfluidic cell culture[†]

Edinson Lucumi Moreno,^a Siham Hachi,^a Kathrin Hemmer,^a Sebastiaan J. Trietsch,^b Aidos S. Baumuratov,^a Thomas Hankemeier,^{b,c} Paul Vulto,^{b,c} Jens C. Schwamborn,^a Ronan M.T. Fleming^a

Received Xth XXXXXXXXXXXX 20XX, Accepted Xth XXXXXXXXXXXX 20XX

First published on the web Xth XXXXXXXXXXXX 200X

DOI: 10.1039/b000000x

A hallmark of Parkinson's disease is the progressive loss of nigrostriatal dopaminergic neurons. We derived human neuroepithelial cells from induced pluripotent stem cells and successfully differentiated them into dopaminergic neurons within phase-guided, three-dimensional microfluidic cell culture bioreactors. After 30 days of differentiation within the microfluidic bioreactors, *in situ* morphological, immunocytochemical and calcium imaging confirmed the presence of dopaminergic neurons that were spontaneously electrophysiologically active, a characteristic feature of nigrostriatal dopaminergic neurons *in vivo*. Differentiation was as efficient as in macroscopic culture, with up to 19% of differentiated neurons immunoreactive for tyrosine hydroxylase, the penultimate enzyme in the synthesis of dopamine. This new microfluidic cell culture model integrates the latest innovations in developmental biology and microfluidic cell culture to generate a biologically realistic and economically efficient route to personalised drug discovery for Parkinson's disease.

Introduction

Although our understanding of the aetiopathogenesis of neurodegeneration has rapidly developed in the past two decades, this has not yet been translated into any neuroprotective treatment. The aetiological diversity of neurodegenerative disease and the estrangement of existing preclinical models from clinical disease are critical issues being addressed within personalised biomedicine. Deriving cells with neuronal phenotypes from patients with neurodegenerative disorders through cellular reprogramming has the potential to revolutionise preclinical disease modelling¹. Human terminally differentiated cells can be reprogrammed to an embryonic-like state through the ectopic expression of only four stem cell transcription factors^{2,3}. The resulting induced pluripotent stem cells (iPSCs) offer a new tool for *in vitro* disease modelling⁴, especially relevant for neurodegenerative diseases as access to human neuronal cells is otherwise difficult. However, developing *in vitro* cellular models to study neurodegenerative diseases requires the use of appropriate neuronal cell types under the right biological, chemical and physical conditions^{5–7}. Efficient neural

induction of iPSCs can be achieved by inhibiting the transforming growth factor beta and bone morphogenetic protein signalling pathways⁸. A combinatorial activation of the antagonising neural plate border pathways WNT and SHH enables the generation and long-term renewal of these cells.

A key pathological feature of Parkinson's disease is the progressive loss of nigrostriatal dopaminergic neurons (DNs)⁹. Starting with fibroblasts obtained from familial or sporadic Parkinson's disease patients, dysfunctional cellular phenotypes are observed in macroscopic *in vitro* cultures of iPSC-derived DN^{10–13}, opening up the possibility to screen for compounds that rescue dysfunctional cellular phenotypes¹². The aforementioned personalised *in vitro* disease models are based on macroscopic, two dimensional culture. Macroscopic culture in this context refers to the use of a macroscopic-scale cell culture device (Petri dish, flasks and multi-well plates). Two dimensional culture cannot reproduce the normal anatomy and physiology of cells designed to live in a three dimensional microenvironment¹⁴. Moreover, macroscopic culture is inefficient with respect to the use of scarce patient derived cellular material and expensive reagents. Medium requirements in such devices ranges from 20 mL for large flasks to 200 μ L for each well of a 96-well plate^{15,16}, requiring the use of proportionate amounts of growth factors.

Reinhardt et al. recently established a protocol, using only small molecules, for derivation and expansion of human neuroepithelial stem cells from human induced pluripotent stem

^a Luxembourg Centre for Systems Biomedicine, University of Luxembourg, 7 avenue des Hauts-Fourneaux, L-4362 Esch-sur-Alzette, Luxembourg. E-mail: ronan.m.fleming@gmail.com

^b Mimetis B.V, PO Box 11002, 2301EA Leiden, The Netherlands.

^c Analytical BioSciences Division, Leiden Academic Centre for Drug Research, Leiden University, Einsteinweg 55, 2333CC Leiden, The Netherlands.

[†] Electronic Supplementary Information (ESI) available: Supplementary movies 1,2 and 3. See DOI: 10.1039/b000000x/

cells or human embryonic stem cells¹³. Using additional growth factors, these neuroepithelial stem cells can be differentiated into neural tube and neural crest lineages, including midbrain-specific DNs that are electrophysiologically functional and integrate after transplantation into the midbrain of adult mice¹³. Reinhardt et al. protocol is well suited for large-scale *in vitro* disease modelling and phenotypic screening as it robustly generates a large and immortal population of neuroepithelial stem cells, obviating the requirement for costly growth factors or cumbersome manual steps. Nevertheless, the subsequent differentiation step does require costly growth factors and to date, it has only been completed in two dimensional macroscopic cell culture¹³ and following transplantation in the brain of mice^{17–19}. Human dopaminergic neurons derived from neural progenitor cells have been macroscopically cultured in 3D neurospheres^{20,21}, but to our knowledge, 3D microfluidic cell culture of iPSC-derived dopaminergic neurons has not yet been reported.

Microfluidic cell culture offers a complementary approach to study neuronal differentiation from induced pluripotent stem cells under controlled experimental conditions²². 3D microfluidic cell culture devices permit the spatio-temporal control over the cellular microenvironment, monitoring of cellular events using current microscopy techniques and perfusion culture to exchange nutrients, growth factors, signalling molecules, waste products and gasses at controlled rates^{23–25}. Microfluidic cell culture comes with many advantages and challenges, determined by the quality of the match between the microfluidic cell culture device and the cell culture phenotype desired¹⁶. Biocompatibility aside, any macroscopic cell culture protocol is the result of heuristic optimisation by generations of biologists and cannot be assumed to be optimal for microfluidic cell culture as the mechanisms of fluid and gas exchange in a microfluidic device will deviate from the exchange typical of macroscopic culture¹⁶.

Trietsch et al. recently described a stratified 3D cell culture bioreactor²⁶. Each bioreactor contains a lane of hydrogel-embedded cells and one or more adjacent lanes of laminarily flowing liquid. Every pair of lanes is partially separated by a phaseguide, which is a geometric feature introduced to pattern liquids flowing into each bioreactor. Each phaseguide induces a meniscus pinning effect that forces an advancing liquid to align itself with the phaseguide instead of flowing over it^{27,28}. To load a bioreactor, cells are mixed with a liquified, surrogate extracellular matrix that is then dispensed into a well connected to a phaseguide delimited lane. Upon gellation this lane becomes the aforementioned lane of gel-embedded cells. Next, fresh media is added to another well that is connected to a media lane adjacent to the gel-embedded cells.

In a typical bioreactor²⁶, a phaseguide is not higher than one fourth of the height of a lane, permitting diffusion between the lane of gel-embedded cells and the fluid media lane(s).

While diffusion will allow the supply of nutrients and efflux of waste metabolites, cells embedded within the gel are shielded from shear stress. Arrays of bioreactors are incorporated in a microtiter plate format, termed an OrganoPlate (Mimetas BV, Leiden), which is fully compatible with standard laboratory automation equipment. The functionality of this platform with respect to 3D culture of immortalised cell lines with continuous perfusion, co-culture and invasion has already been established²⁶, but not yet for differentiation of induced pluripotent stem cell-derived cell lines.

Hydrogels are often used as a surrogate extracellular matrix for 3D culture because of their biomechanical properties. They provide mechanical integrity, yet permit the diffusion of signalling molecules, nutrients and metabolic wastes²⁹. Natural hydrogels, e.g. Matrigel, fibrin gel or alginate gel, are composed of proteins and extracellular matrix components³⁰ that provide a suitable extracellular matrix environment for 3D cell culture and endogenous factors that promote, proliferation and development. Synthetic hydrogels like poly(ethylene glycol), poly(vinyl alcohol) and poly(2-hydroxy ethyl methacrylate) act as a template for cell culture, but they lack endogenous factors^{29,30}. A combination of natural and synthetic polymers, e.g., poly(ethylene glycol) and collagen can be used as cell entrapping material²⁹. A commonly used natural hydrogel is BD Matrigel, a reconstituted basement membrane preparation extracted from the Engelbreth-Holm-Swarm (EHS) mouse sarcoma, a tumour rich in extracellular matrix proteins. Matrigel is constituted of 60% laminin, 30% type IV collagen and 8% entactin, in addition to growth factors and other molecules. Entactin acts as a bridging molecule that interacts with laminin and collagen IV contributing to the structural organisation of Matrigel as an extracellular matrix. Interaction of cells in culture with the surrounding extracellular matrix is an active process. Cultured cells may respond to their local environment remodelling the extracellular matrix by synthesising new extracellular matrix or degrading it by the action of extracellular enzymes³¹.

In this paper, we report the successful integration of advanced developmental cell biology and microfluidic cell culture technology. We efficiently differentiated human iPSC-derived neuroepithelial stem cells¹³ into functional DNs within phase-guided 3D cell culture bioreactors²⁶. After 30 days in culture, we confirmed known phenotypic characteristics of DNs by calcium imaging and immunofluorescence. 3D image analysis revealed mature neurons that possessed long neurites showing an interconnected neuronal population. This paper establishes that phase-guided 3D cell culture bioreactors can be successfully integrated with cellular reprogramming of neuroepithelial stem cells to produce an *in vitro* dopaminergic neuronal cell culture model. This model is robust, cost efficient, physiologically proximal and ready for parallelism by laboratory automation, and personalisation by supply of pa-

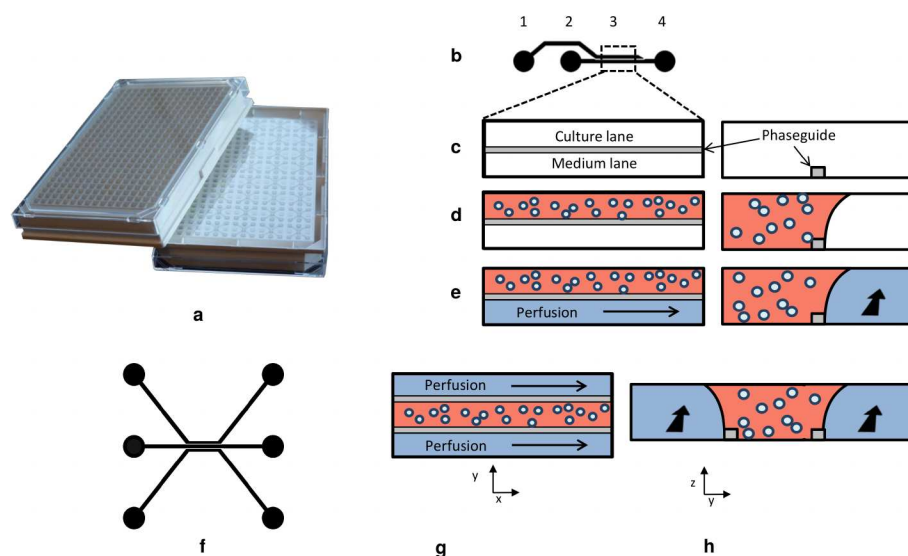


Fig. 1 OrganoPlate concept and filling procedure: (a) A top and bottom view of a 3-lane OrganoPlate. The top is based on a 384-well microtiter plate format, while the bottom consists of 40 microfluidic bioreactors each with one culture chamber. (b) Scheme of a single 2-lane bioreactor comprised of a gel inlet (1), a perfusion inlet (2), an optical readout window (3) and a perfusion outlet (4). (c) A horizontal view of the readout window and a cross section thereof. The 2-lane culture chamber is separated by a phaseguide to allow selective gel patterning. (d) Cells are loaded within liquefied gel and selectively patterned in the culture lane by the phaseguide. (e) Upon gelation, medium is introduced in the perfusion lane and perfusion is driven by gravitational leveling between a perfusion inlet well and a perfusion outlet well. (f) 3-lane bioreactor consisting of two perfusion lanes and one culture lane; (g) gel-embedded cells are perfused from two sides; (h) vertical cross sectional view of (g).

tient derived iPSC from dedicated bio-banks.

Materials and Methods

Microfluidic device

Cells were cultured in 2-lane and 3-lane *OrganoPlates* (Mimetas BV, Leiden, The Netherlands) consisting of arrays of microfluidic bioreactors in a microtiter plate format, detailed previously²⁶ (Fig. 1). In brief, a 2-lane OrganoPlate consists of an array of 96 bioreactors. Each culture chamber is juxtaposed to 4 wells of a 384 well plate with one *gel inlet well* (Fig. 1b, 1) for loading gel-embedded cells into the culture lane, one *readout window* (Fig. 1b, 3) for monitoring the culture lane by inverted light microscopy. In addition, each bioreactor has a *perfusion inlet well* (Fig. 1b, 2) connected to a *perfusion outlet well* (Fig. 1b, 4) via a media perfusion lane, where flow of fluid driven by gravity. In each culture chamber, during cell loading a *phaseguide* prevents liquefied gel-embedded cells from leaving the culture lane and entering the medium lane (Fig. 1 c-e). A phaseguide is a patterned pinning barrier that controls the liquid-air interface by forcing it to align with the ridge and therefore allowing the filling of microfluidic structures²⁷ (Supplementary movie 1). 2- and 3-lane OrganoPlates are the same, except that the latter con-

sists of an array of 40 bioreactors, each of which contains one culture chamber, composed of three lanes separated by two phaseguides (Fig. 1 f-h). This gives more options for stratified culture as only one lane must be used for media perfusion and only one culture lane must be used for gel-embedded cells, the third can be used for either purpose.

Human neuroepithelial stem cell culture

Human neuroepithelial stem cells (hNESCs) derived from iPSC were maintained and differentiated into DNs by adapting an existing protocol described in detail by Reinhardt et al.¹³. We summarise this protocol and highlight any adaptation for microfluidic cell culture. Small molecules (Ascorbic Acid, CHIR, PMA and dbcAMP) and specific growth factors (BDNF, GDNF and TGF β 3) are used to differentiate hNESC into midbrain specific DNs. The culture preparation medium *N2B27 medium* consisted of equal amounts of Neurobasal medium (Life technologies) and DMEM/F12 medium (Life technologies) supplemented with 1% penicillin/streptomycin (Life technologies), 2 mM L-glutamine (Life technologies), 1:100 B27 supplement without Vitamin A (Life technologies) and 1:200 N2 supplement (Life technologies). hNESCs were maintained and proliferated in N2B27 medium up to 70% confluence to have enough cell material to load into wells of the

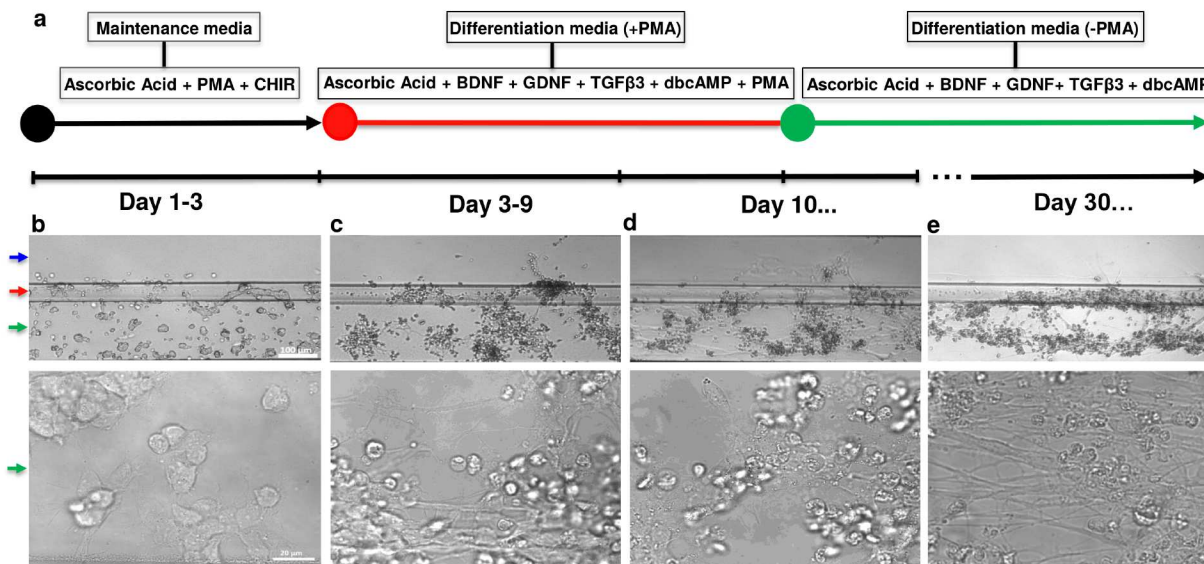


Fig. 2 Differentiation of hNESC into DA neurons. (a) Media components. Bright field images of hNESC in the 2-lane Organoplate (b) 1 day (c) 4 days and (d) 10 days after seeding. (e) hNESC differentiated into neurons in the 2 lane microfluidic culture chamber after 1 month differentiation. Scale bar 100 μm and 20 μm . The blue, red and green arrows on the left indicate the medium lane, phaseguide and culture lane respectively

OrganoPlate.

Dopaminergic neuronal differentiation

The *maintenance medium* to maintain the hNESC in culture consisted of N2B27 medium with 0.5 μM PMA (Enzo life sciences), 3 μM CHIR (Axon Medchem) and 150 μM Ascorbic Acid (Sigma Aldrich). This medium was used to prepare the hNESC at an average cell density of 7 million cells/ml. Corning Matrigel hESC-qualified matrix catalogue number 354277, lot number 3318549 (Discovery Labware) at 50% from reconstituted stock, with cell suspension in maintenance medium, was used as extracellular matrix. hNESC in maintenance medium was mixed with an equal amount of Matrigel and 1 μL of this mix was loaded into each inlet wells of 2-lane (2 μL in the 3-lane) microfluidic bioreactors in an OrganoPlate, using a repeating pipette (Eppendorf) following the plate loading protocol previously described by Trietsch et al.²⁶. In each microfluidic bioreactor, the hNESC are embedded within Matrigel adjacent to one or more perfusion lane, rather than seeded on top of Matrigel with media above, as in the macroscopic culture protocol reported by Reinhardt et al.¹³. After loading cells into culture chambers of the OrganoPlate, the plate was incubated at 37 $^{\circ}\text{C}$ and 5% CO_2 for 10 min to allow initial gelation of Matrigel. To start medium perfusion by gravity, maintenance medium was added to perfusion inlet and outlet wells where an average fluid flow

of 1.5 $\mu\text{L h}^{-1}$ is achieved²⁶.

The *differentiation medium with PMA* to induce the differentiation of hNESC towards DN, consisted of N2B27 medium with 200 μM ascorbic acid, 0.01 $\text{ng}/\mu\text{L}$ BDNF (Peprotech), 0.01 $\text{ng}/\mu\text{L}$ GDNF (Peprotech), 0.001 $\text{ng}/\mu\text{L}$ TGF β 3 (Peprotech), 2.5 μM dbcAMP (Sigma Aldrich) and 1 μM PMA. Differentiation medium with PMA was changed, every 2 days during the first 6 days of culture in the differentiation process.

For the maturation of differentiated neurons, PMA was no longer added to the differentiation medium, *differentiation medium without PMA*, from day 7 onwards, this differentiation medium without PMA was changed every 2 days during 3 weeks. Exchange of differentiation medium with and without PMA was done 3 times a week to ensure the stability of small molecules used during the differentiation process.

To monitor cellular morphology during differentiation, bright field images were acquired using a Zeiss Axiovert 40 CFL microscope equipped with a cooled CCD camera (Zeiss AxioCam Mrm, Zeiss).

Calcium imaging

A calcium imaging assay was done on representative wells. 80 μL of 5 μM cell permeant Fluo-4 AM (Life technologies) in neurobasal medium was added to inlet wells of microfluidic bioreactors at room temperature. Fluorescence images

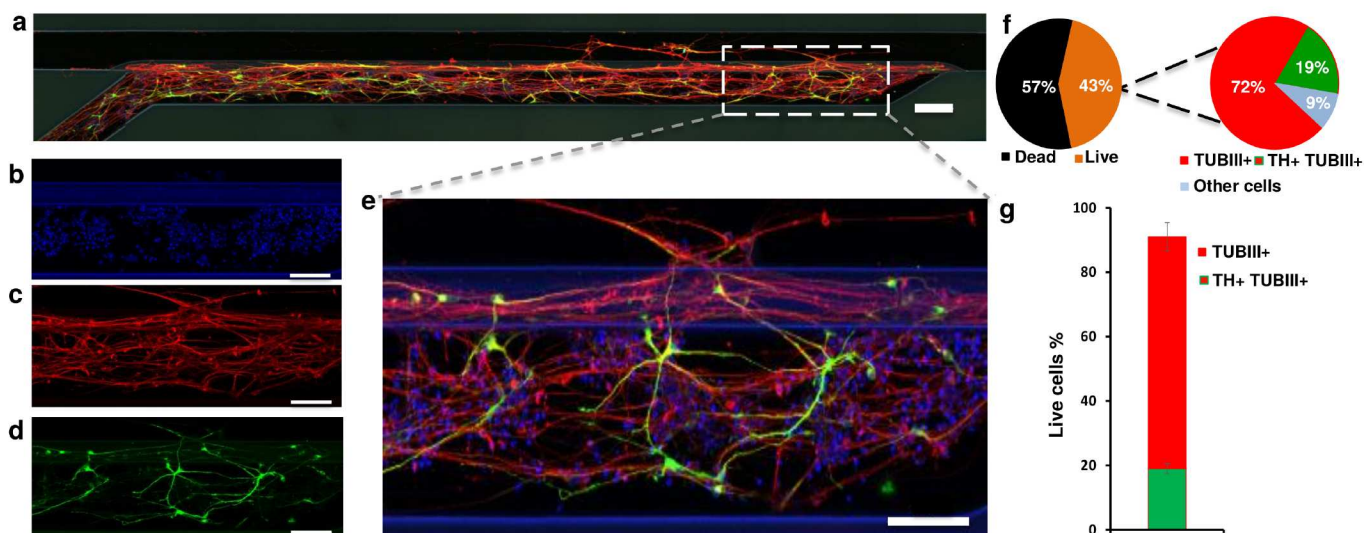


Fig. 3 Differentiation of hNESC into neurons in 2-lane microfluidic bioreactor of the OrganoPlate. (a) Immunostaining of differentiated neurons in 2-lanes microfluidic chamber after 1 month differentiation, scale bar 200 μm . Section of microfluidic chamber stained for (b) Nuclei with Hoechst in blue. (c) TUB β III in red. (d) TH in green, scale bar 50 μm . (e) Merged nuclei, TUB β III and TH stains, scale bar 100 μm . (f) Efficiency of survival and differentiation of hNESC into neurons. (g) Efficiency of TH positive neurons (DNs), error bars show standard deviation from 3 different bioreactors of the 2-lane OrganoPlate.

were acquired using an epifluorescence microscope (Leica DMI6000B) equipped with a cooled sCMOS camera (Neo 5.5, Andor technology) with both apparatus controlled with Micro-manager (version 1.4)³². Images were sampled at a rate of 8.4 Hz for ~ 2 min, stored as image stacks and analysed using custom Matlab (version 2013b; MathWorks) scripts. Fluorescence traces were extracted from manually segmented regions of interest corresponding to neuronal cell bodies and were presented as relative changes in fluorescence ($\Delta F/F$). Thereafter, the most probable spike train was inferred from fluorescence observations using a fast non-negative deconvolution algorithm described by Vogelstein et al.³³. The output of this algorithm is the probability that a spike occurred in a given time frame. In order to binarise the resulting spike train (1 for neuron activated and 0 for neuron not activated), we thresholded the vector of probabilities \mathbf{v} such that the spikes with a probability below $2/3(\min(\mathbf{v}) + \max(\mathbf{v}))$ were set to 0 and the remaining ones were set to 1. Thus, spikes with the highest probabilities indicated the activation of the neuron.

Immunofluorescence staining

The *in vitro* dopaminergic phenotype is characterised by the expression of specific neuronal markers, TUB β III and tyrosine hydroxylase (TH), the rate limiting enzyme in the biosynthesis of dopamine^{13,34,35}. Immunostaining for TH positive cells was performed on representative wells at day 30 of differenti-

ation. Differentiated cells were fixed with 4% paraformaldehyde (PFA) in 1 \times phosphate-buffered saline (PBS) for 15 min, followed by permeabilisation with 0.05% Triton-X 100 in 1 \times PBS (3 min on ice), and blocking with 10% fetal calf serum (FCS) in 1 \times PBS (1h). After washing with 1 \times PBS, the primary antibodies mouse anti-TUB β III (1:2000, Covance) and rabbit anti-TH (1:2000, Santa cruz biotechnology), were incubated for 90 min at room temperature. After washing with 1 \times PBS, the secondary antibodies Alexa Fluor 488 Goat Anti-Rabbit and Alexa Fluor 568 Goat Anti-Mouse together with a stain DNA (Hoechst 33342, Invitrogen), were incubated overnight at 4 $^{\circ}\text{C}$ on a rotary shaker. After washing with 1 \times PBS, confocal images of representative culture chambers were acquired using a confocal microscope (Zeiss LSM 710). After confocal images were acquired, a spot detection algorithm (Imaris software, Bitplane) was used to detect and count nuclei in order to be able to calculate the efficiency of differentiation (see Supplementary data for more details).

Results

Differentiation of human neuroepithelial stem cells into neurons in microfluidic cell culture

The protocol to differentiate hNESC into DNs was successfully implemented in 2-lane and 3-lane OrganoPlates using maintenance and differentiation media as depicted in Fig. 2a.

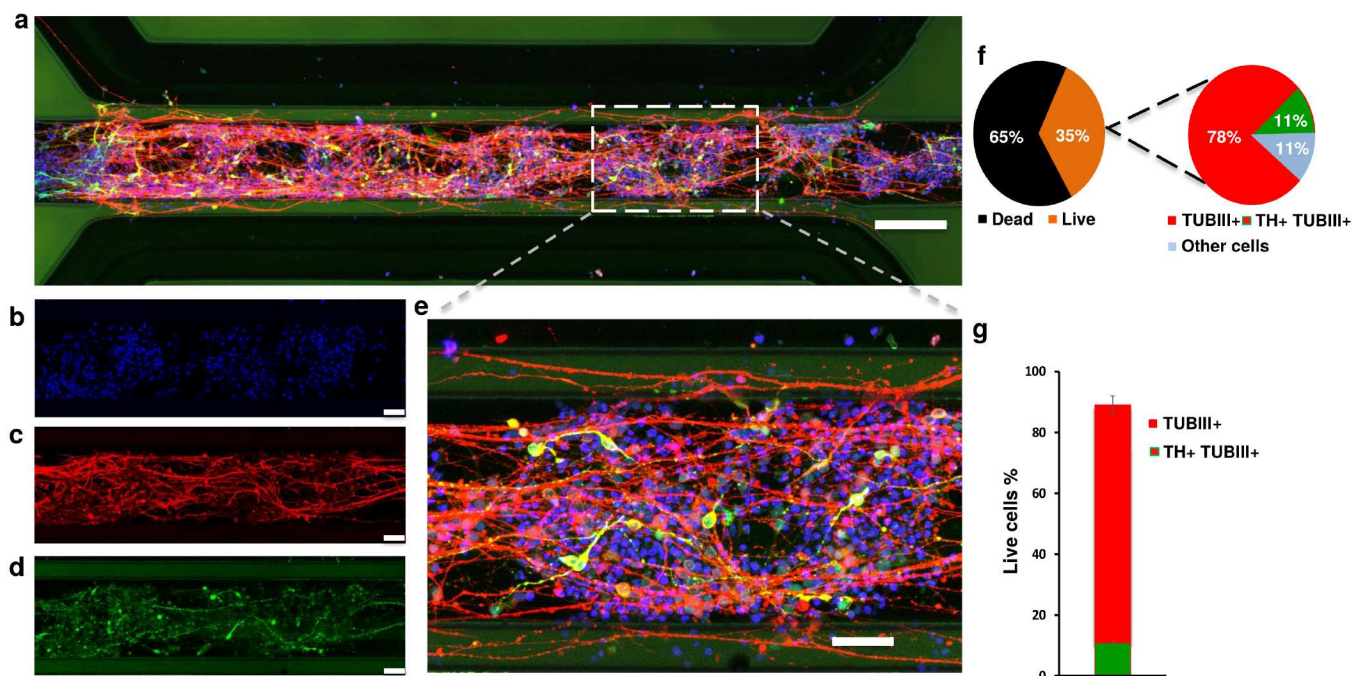


Fig. 4 Differentiation of hNESC into neurons in 3-lane microfluidic bioreactor of the OrganoPlate. (a) Immunostaining of differentiated neurons in 3-lanes microfluidic chamber after 1 month differentiation, scale bar 200 μm . Section of microfluidic chamber stained for (b) Nuclei with Hoechst, (c) TUB β III, (d) TH, scale bar 50 μm and (e) Merged nuclei, TUB β III and TH stains, scale bar is 100 μm . (f) Correlation of live dead regarding differentiation of hNESC into neurons and efficiency of differentiation (g) Efficiency of TH positive (mDN) neurons, error bars show standard deviation from 3 different bioreactors of the 3 lanes OrganoPlate.

Three hours after loading Matrigel-embedded hNESC into the OrganoPlate, small cellular aggregates started to form. Cells in these aggregates started to project plasma membrane protrusions (filopodia)³⁶ to probe their new microenvironment, during perfusion with maintenance medium and incubation at 37 °C (Fig. 2b). During the days of exposure to differentiation medium with PMA (day 3 to 10), the morphology of hNESC was mainly characterised by the extension of those protrusions into more neurite-like structures. In addition to a more defined polarisation (unipolar and bipolar)³⁷ of the differentiated hNESC, growth cones and additional filopodia arise from the main neurite³⁸ (supplementary figure 1). Furthermore, proliferating and dead hNESC can be observed in the culture chamber (Fig. 2c). Maturation of differentiating hNESC into a more robust neuron like phenotype was started by using differentiation medium without PMA (Fig. 2d). Differentiating neurons were kept maturing and differentiating for 21 additional days. Throughout this maturation stage, the differentiated neurons had more defined bipolar morphology, growth cones, varicosities and larger neurites processes, typical of a more mature neuronal phenotype (Fig. 2e) (Supplementary Figure 1).

Characterisation of differentiated neurons

2-lane OrganoPlate In 2-lane bioreactors, differentiated neurons were identified by immunoreactivity for the marker TUB β III (red, Fig. 3). The staining of differentiated neurons positive for TUB β III showing the neurite distribution, outreach and ramification in this selected area of the culture lane can be seen in Fig. 3c. Dopaminergic neurons exhibited a spatially homogeneous distribution along the length and breadth of the lane (Fig. 3a). A closer look into the selected area highlighted in Fig. 3a, shows the staining of nuclei with Hoechst (blue, Fig. 3b). Differentiated neurons positive for TH confirmed the presence of DNs as shown in Fig. 3d. An enlarged view of the merged image of stained neurons in a selected area in the culture lane is shown in Fig. 3e.

The 2- and 3-lane OrganoPlate consists of 96 and 40 bioreactors respectively. Once the hNESC were loaded to the culture chamber, they had to adapt to the new 3D microenvironment. After 48 hours in culture, approximately 70% of 2- and 3-lane bioreactors had culture chambers with viable cells. A possible factor contributing to this decrease in bioreactors with viable cells could be the temperature changes experienced by the cells during the sample preparation step, premature gelation of Matrigel and medium evaporation from wells located

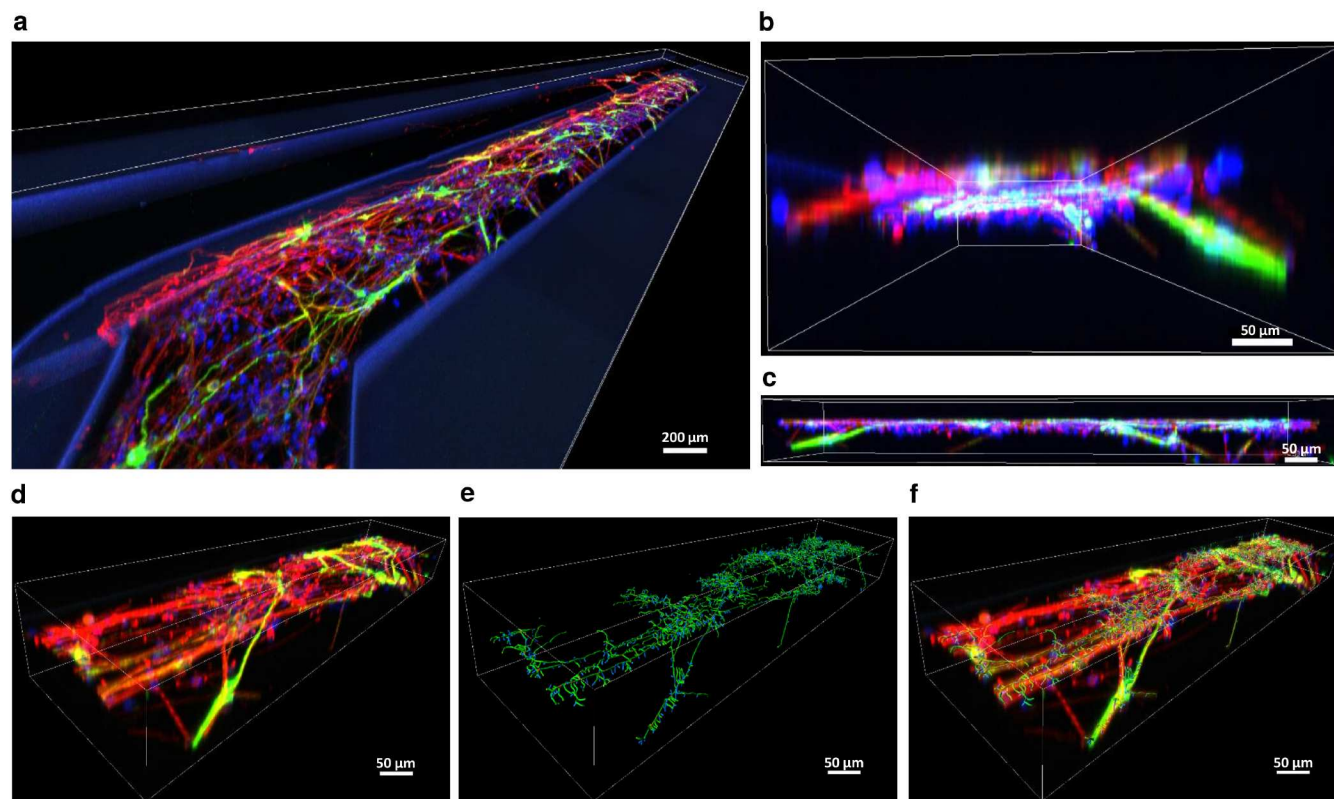


Fig. 5 3D representation and distribution of TH positive differentiated neurons in 2-lane microfluidic culture chamber of the OrganoPlate. (a) Top view of entire culture chamber, scale bar 200 μm . (b) Inside view and (c) side view of a selected area of the culture lane, scale bar 50 μm . (d) Top view of selected area, (e) reconstruction of neuronal filaments of TH and TUB β III-positive neurons in a selected area, (f) Overlap of (d) and (e), scale bar 50 μm .

at the edge of the plate. In this study, we used cell counts for 3 typical bioreactors in the 2-lane OrganoPlate to calculate the average survival rate in bioreactors with viable cells during the differentiation process. Approximately half of all cells die in a typical culture lane. Of the live cells, 91% differentiated into TUB β III positive cells, indicating highly efficient neuronal differentiation (Fig 2f). 9% of live cells were negative for both TUB β III and TH, indicating either a failure to differentiate or differentiation into non-neuronal lineages. Of the live cells, 72% were positive only for TUB β III and 19% were positive for both TUB β III and TH (Fig 2f), indicating efficient differentiation into dopaminergic neurons (Fig. 3g).

3-lane OrganoPlate In 3-lane bioreactors, Matrigel-embedded cells were flanked by two media perfusion lanes. A homogeneous distribution of differentiated neurons was observed throughout the length and breadth of typical culture lanes (Fig. 4a). Similar to Fig. 3b, the spatial distribution of cell nuclei (Hoechst staining) in a selected area of the culture lane is illustrated in Fig. 4b, neurites (TUB β III staining) in Fig. 4c, neurons positive for TH are shown in Fig. 4d and

an enlarged view of a selected area of the culture lane showing the merged distribution of used cellular markers of differentiated neurons is shown in Fig. 4e.

In cell culture lanes of the 3-lane OrganoPlate, 65% of cells died during the differentiation process. Out of the 35% surviving cells, 11% were negative for TUB β III and TH (undifferentiated remaining neural stem cells). Among the remaining 89% of cells differentiated into neurons, 78% were only positive for TUB β III and 11% were positive for TUB β III and TH as shown in Fig. 4f. The efficiency of TH positive neuronal differentiation in the bioreactors of the 3-lane OrganoPlate was therefore 11% (Fig. 4e).

3D distribution of differentiated dopaminergic neurons

A 3D reconstruction of differentiated neurons in a representative culture chamber of a 2-lane OrganoPlate revealed the distribution of differentiated neurons positive for TUB β III and TH (Fig. 5a). Both medium perfusion and cell culture lanes can be seen, separated by a phaseguide, demonstrating that

cells are confined to the culture lane. A longitudinal view along the same culture lane revealed that many cells had migrated toward the top of the Matrigel (Fig. 5b). Furthermore the upper surface of the Matrigel no longer reached the top of the culture lane, rather it had contracted to create an apparently concave upper surface. A side view of the same culture lane shows the spatial localization of neurite projections relative to the height of the channel (Fig. 5c). The top side view orientation of differentiated cells in the channels shows the level of connectivity among TUB β III and TH positive neurons (Fig. 5d).

Surface reconstruction and filament tracing revealed a truly three-dimensional distribution of differentiated cells in the culture lane, as shown in Fig. 5e and Supplementary movie 2. An overlay of the neuronal distribution and the filament reconstruction of neurons located in this area of the plate shows the high level of branching, interconnectivity and the length of neurites of differentiated neurons (Fig. 5f).

Electrophysiological activity of differentiated neurons

Analysis of calcium imaging time-series of representative culture chambers revealed spontaneous neuronal activity in several differentiated neurons. A calcium transient, evoked by an action potential, is characterised by a fast rise in intracellular calcium concentration due to neuronal depolarisation followed by a slower exponential decay corresponding to the slow unbinding rate of calcium ions from the fluorescent probe^{39,40}. Fig. 6 shows somatic fluorescence signals extracted from spontaneously active neurons in a 3-lane OrganoPlate, where calcium transients evoked by action potentials were visible (see also Supplementary movie 3).

Fig. 6a depicts the mean fluorescence image of a TH immunoreactive differentiated neuron. Using the Fluo-4 fluorescence trace of this neuron, we applied the algorithm reported by Vogelstein et al.³³ to infer the most probable spike train underlying the trace (Fig. 6b). Interestingly, the resulting spontaneous calcium transients and the underlying spikes tend to be regular and this is consistent with previous *in vitro* studies on the tonic electrophysiological activity of DNs^{41,42}. Fig. 6c-e illustrate fluorescence traces and inferred spike trains from three different TH-negative neurons. These results show that TH-negative neurons tend to depolarise in more irregular temporal patterns than TH-positive cells. Fig. 7 shows calcium signals extracted from the soma, neurite and neurite terminal of a typical electrophysiologically active neuron in a culture chamber of a 2-lane OrganoPlate. At our sampling rate of 8.4 Hz, calcium transients appeared to be synchronised between these three regions, indicating that each action potential does propagate along neurites.

Discussion

The degeneration of substantia nigra dopaminergic neurons is one of the hallmarks of Parkinson's disease⁴³. The efficient generation of iPSC-derived dopaminergic neuronal *in vitro* cultures with phenotypic properties proximal to those observed *in vivo* in patients and matched controls, is therefore an important goal for personalised biomedicine approaches to Parkinson's disease. We successfully differentiated human neuroepithelial stem cells (hNESCs) into dopaminergic neurons within established microfluidic cell culture bioreactors²⁶. In each bioreactor, a 3D lane of Matrigel-embedded cells is flanked by bulk flow of fluid medium on one or both sides. Human neuroepithelial stem cells (hNESCs) were derived from iPSC using an established macroscopic cell culture protocol that only requires small molecules¹³. Differentiation of hNESC into midbrain-specific dopaminergic neurons requires the use of expensive reagents. Our use of these reagents in microfluidic cell culture is approximately 10 times less than in macroscopic culture, making microfluidic culture more economical.

The calculation of the percentage of dead cells in the culture is based on counting nuclei (Hoechst stain) in the culture lane. The percentage of dead cells reflects the prevalence of cell death after a 30 day culture period, because dead gel-embedded cells are not flushed out by renewal of media. This is in contrast to two dimensional macroscopic culture where one typically measures the incidence of cell death between media renewals, each of which flushes away dead cells that detach from the underlying culture surface. Differentiation efficiency has been observed to increase in a sigmoidal fashion with time¹³. After 30 days exposure to differentiation media, we achieved an immunocytologically confirmed neuronal differentiation efficiency of 91%, which compares favourably with the 50% efficiency observed in macroscopic culture after 21 days¹³. The remaining cells (TUB β III negative, TH negative) are either undifferentiated hNESC or astrocytes as observed in macroscopic culture and suggested by phase contrast images indicating astrocytic morphology (Data not shown). Of the immunocytologically confirmed neurons, dopaminergic neuronal differentiation efficiency was 19% and 11% within 2- and 3-lane microfluidic bioreactors respectively, compared to 30% efficiency observed in macroscopic culture after 21 days¹³. Gel-embedded cells in a 3-lane bioreactor are flanked by media perfusion on two sides, as opposed to one side in a 2-lane bioreactor. The lower differentiation efficiency in 3-lane bioreactors may be due to increased dilution of paracrine factors suggesting that modulation of the media perfusion rate could lead to higher differentiation efficiency.

In mouse⁴¹ and guinea-pig⁴² brain slices, nigrostriatal dopaminergic neurons exhibit spontaneous firing, at a highly regular rate. Our calcium imaging, acquired *in situ*, con-

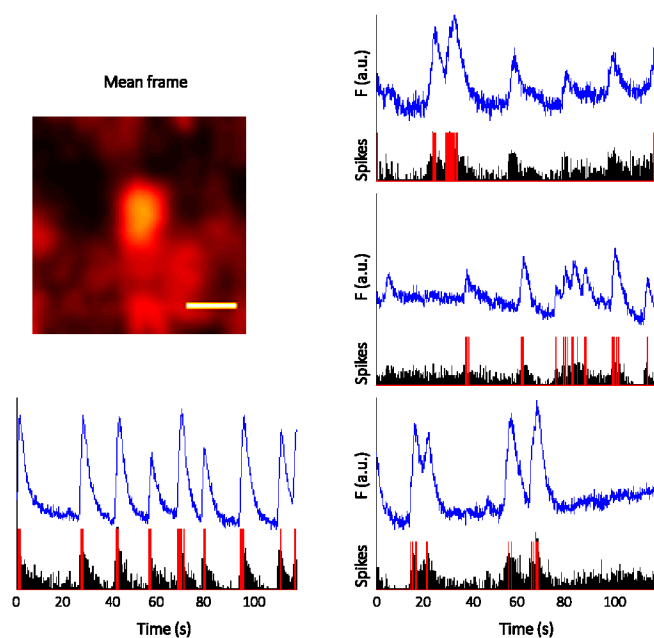


Fig. 6 Monitoring of spontaneous neuronal activity of differentiated neurons in culture chamber of the 3-lane OrganoPlate. (a) Mean frame of a field of view representing an electrophysiologically active TH immunoreactive neuron, scale bar 20 μm . (b) Fluorescence trace (blue line) and the inferred spike train corresponding to the neuron in (a) (black bars using the fast nonnegative deconvolution filter and red bars after thresholding). (c-e) Fluorescence traces corresponding to three different non TH positive neurons and the underlying spike trains.

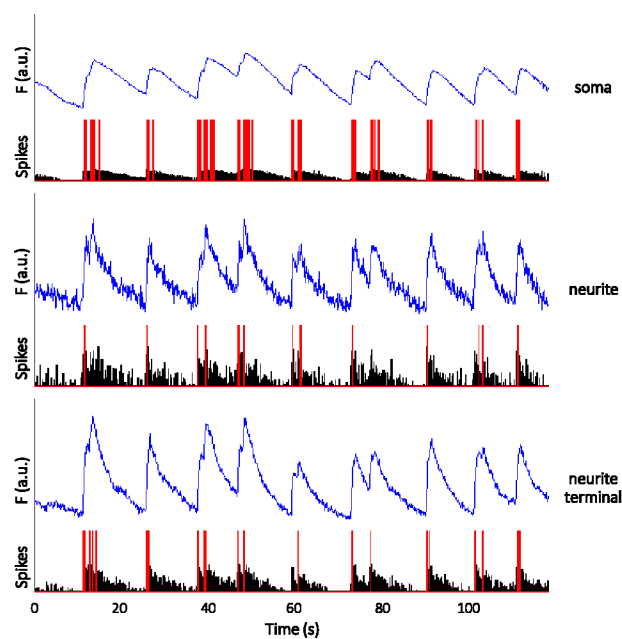


Fig. 7 Fluorescence traces (blue lines) and the inferred spike trains corresponding to different regions of a differentiated neuron in culture chamber of the 2-lane OrganoPlate (black bars using the fast nonnegative deconvolution filter and red bars after thresholding). (a) soma (b) neurite (c) neurite terminal.

firmed spontaneous electrophysiological activity in differentiated neurons, with action potentials propagating along neurites. A more regular firing pattern was observed in dopaminergic neurons (TUB β III and TH positive cells) as opposed to other neurons (TUB β III positive, TH negative) indicating that these cells are electrophysiologically more proximal to nigrostriatal dopaminergic neurons *in vivo*. We employed a deconvolution algorithm³³ to infer the probability of a depolarisation event underlying successive intervals of the calcium signal. Patch clamp recordings, in parallel to calcium imaging from individual hNESc-derived dopaminergic neurons, would be required to tune the free parameters of the deconvolution algorithm and express greater confidence in the predicted depolarisation events since nigrostriatal dopaminergic neurons are known to exhibit atypically broad action potentials⁴⁴.

Our results reinforce the previously observed biocompatibility of the materials used in our phase-guided 3D cell culture bioreactors (OrganoPlate, Mimetas BV). This is important because assays of biocompatibility must be completed with a range of cell types as different cell types do respond differently to the same cell culture device⁴⁵. This is especially so with microfluidic cell culture, where the ratio between cellular volume and culture device surface area (in diffusive contact with cells) is typically much lower than for macroscopic culture⁴⁶. We use a phaseguide to separate media and culture lanes that is 1/4 of the height of the lane, therefore at least 3/4 of the surface area of the gel in the culture lane is in diffusive contact with fresh media. This provides ample supply of fresh nutrients and dissolved gasses and avoids any requirement for micro fabricated pillar arrays or other barriers to nutrient exchange.

Reinhardt et al.¹³ used Matrigel to coat the surface of macroscopic culture plates upon which hNESc were cultured. In contrast, we first mixed hNESc with fluid Matrigel at 4 °C, then dispensed this mix from a pipette into a cooled bioreactor. This mix gellates when the temperature of the bioreactor rises above 10 °C. This loading step requires careful control over temperature to ensure that the mix remains fluid until lane loading is complete. We have observed that premature gellation lowers cell viability. This may be due to increased viscosity of a partially gellated mix which would result in shear stress to embedded cells during loading. After gellation, hNESc should have an isotropic cellular morphology with any anisotropy indicative of shear stress during loading. Regarding the ratio of live:dead cells, it is hard to obtain comparable data from macroscopic 2D culture where dead cells detach and are flushed away by media replacement. In contrast, dead cells continue to reside *in situ* within our 3D culture.

While maintaining Matrigel at 4 °C keeps it fluid, 37 °C is the optimal temperature for culture of most human cells. Mixing hNESc with fluid Matrigel at 4 °C does expose them to a cold shock⁴⁷ that must be as long as the loading of all

desired bioreactors on a single microfluidic plate. Of the microfluidic bioreactors loaded with hNEScs, approximately 7 out of 10 culture chambers had aggregates of viable cells after 48h in culture. It may be that the cold shock experienced by the hNESc contributes to the collective loss of viability in non-viable chambers, though some loss of collective viability is also normally expected amongst any set of macroscopic culture wells. Future experiments are required with alternatives to Matrigel that can suspend cells in fluid during loading, gellate in a controlled manner without harming embedded cells and yet act as a biocompatible extracellular matrix upon gellation.

Conclusions

We successfully differentiated human neuroepithelial stem cells into dopaminergic neurons within phase-guided, three dimensional microfluidic cell culture bioreactors. After 30 days of differentiation, *in situ* morphological, immunocytological and electrophysiological characterisation of dopaminergic neurons confirmed the biological fidelity of this new *in vitro* model and emphasised the biocompatibility of this phase-guided microfluidic device.

Each microfluidic bioreactor requires a fraction of the expensive reagents typical of macroscopic culture and our arrays of microfluidic bioreactors are arranged in a microtitre-plate format that is compatible with standard laboratory automation. These features, combined with the establishment of biobanks of patient-derived induced pluripotent stem cells, provide an efficient route to personalise industrial-scale drug discovery.

Acknowledgements

The authors thank Inga Werthschulte for the technical support on providing the hNESc used in all experiments. AFR (Aides la Formation-Recherche) Training allowance to Edinson Lucumi Moreno from FNR (Fonds National de la Recherche Luxembourg). A Pelican award from the Fondation du Pelican de Mie et Pierre Hippert-Faber supported KH. The JCS lab is supported by a CORE grant from the Fonds National de la Recherche.

References

- 1 F. Ali, S. R. W. Stott and R. A. Barker, *Experimental Neurology*, 2014, **260**, 3–11.
- 2 J. Yu, M. A. Vodyanik, K. Smuga-Otto, J. Antosiewicz-Bourget, J. L. Frane, S. Tian, J. Nie, G. A. Jonsdottir, V. Ruotti, R. Stewart, I. I. Slukvin and J. A. Thomson, *Science*, 2007, **318**, 1917–1920.
- 3 K. Takahashi, K. Tanabe, M. Ohnuki, M. Narita, T. Ichisaka, K. Tomoda and S. Yamanaka, *Cell*, 2007, **131**, 861–872.
- 4 M. Bellin, M. C. Marchetto, F. H. Gage and C. L. Mummery, *Nat Rev Mol Cell Biol*, 2012, **13**, 713–726.

- 5 R. Gonzalez, I. Garitaonandia, T. Abramihina, G. K. Wambua, A. Ostrowska, M. Brock, A. Noskov, F. S. Boscolo, J. S. Craw, L. C. Laurent, E. Y. Snyder and R. A. Semchkin, *Sci. Rep.*, 2013, **3**, 1463.
- 6 J. N. L. Grand, L. Gonzalez-Cano, M. A. Pavlou and J. C. Schwamborn, *Cell. Mol. Life Sci.*, 2014, 1–25.
- 7 A. Swistowski, J. Peng, Q. Liu, P. Mali, M. S. Rao, L. Cheng and X. Zeng, *STEM CELLS*, 2010, **28**, 1893–1904.
- 8 S. M. Chambers, C. A. Fasano, E. P. Papapetrou, M. Tomishima, M. Sadelain and L. Studer, *Nature Biotechnology*, 2009, **27**, 275–280.
- 9 H. Braak and K. Del Tredici, *Adv Anat Embryol Cell Biol*, 2009, **201**, 1–119.
- 10 H. N. Nguyen, B. Byers, B. Cord, A. Shcheglovitov, J. Byrne, P. Gujar, K. Kee, B. Schüle, R. E. Dolmetsch, W. Langston, T. D. Palmer and R. R. Pera, *Cell Stem Cell*, 2011, **8**, 267–280.
- 11 A. Sanchez-Danes, Y. Richaud-Patin, I. Carballo-Carbajal, S. Jimenez-Delgado, C. Caig, S. Mora, C. Di Guglielmo, M. Ezquerro, B. Patel, A. Giralt, J. M. Canals, M. Memo, J. Alberch, J. Lopez-Barneo, M. Vila, A. M. Cuervo, E. Tolosa, A. Consiglio and A. Raya, *EMBO Mol Med*, 2012, **4**, 380–395.
- 12 O. Cooper, H. Seo, S. Andrabi, C. Guardia-Laguarta, J. Graziotto, M. Sundberg, J. R. McLean, L. Carrillo-Reid, Z. Xie, T. Osborn, G. Hargus, M. Deleidi, T. Lawson, H. Bogetofte, E. Perez-Torres, L. Clark, C. Moskowitz, J. Mazzulli, L. Chen, L. Volpicelli-Daley, N. Romero, H. Jiang, R. J. Uitti, Z. Huang, G. Opala, L. A. Scarffe, V. L. Dawson, C. Klein, J. Feng, O. A. Ross, J. Q. Trojanowski, V. M.-Y. Lee, K. Marder, D. J. Surmeier, Z. K. Wszolek, S. Przedborski, D. Krainc, T. M. Dawson and O. Isacson, *Sci Transl Med*, 2012, **4**, 141ra90.
- 13 P. Reinhardt, M. Glatz, K. Hemmer, Y. Tsytysyura, C. S. Thiel, S. Honing, S. Moritz, J. A. Parga, L. Wagner, J. M. Bruder and e. al, *PLoS ONE*, 2013, **8**, e59252.
- 14 J. W. Haycock, in *3D Cell Culture*, ed. J. W. Haycock, Humana Press, 2011, pp. 1–15.
- 15 A. L. Paguirigan and D. J. Beebe, *Bioessays*, 2008, **30**, 811.
- 16 S. Halldorsson, E. Lucumi, R. Gómez-Sjöberg and R. M. T. Fleming, *Biosens. Bioelectron.*, 2015, **63C**, 218–231.
- 17 G. Hargus, O. Cooper, M. Deleidi, A. Levy, K. Lee, E. Marlow, A. Yow, F. Soldner, D. Hockemeyer, P. J. Hallett, T. Osborn, R. Jaenisch and O. Isacson, *Proceedings of the National Academy of Sciences of the United States of America*, 2010, **107**, 15921–15926.
- 18 K. Hemmer, M. Zhang, T. van Wüllen, M. Sakalem, N. Tapia, A. Baumuratov, C. Kaltschmidt, B. Kaltschmidt, H. R. Schöler, W. Zhang and J. C. Schwamborn, *Stem Cell Reports*, 2014, **0**, year.
- 19 G. Hargus and e. al, *Cell reports*, 2014, **8**, 1697–1703.
- 20 C. Brito, D. Simão, I. Costa, R. Malpique, C. I. Pereira, P. Fernandes, M. Serra, S. C. Schwarz, J. Schwarz, E. J. Kremer and P. M. Alves, *Methods*, 2012, **56**, 452–460.
- 21 E. J. Gualda, D. Simao, C. Pinto, P. M. Alves and C. Brito, *Front Cell Neurosci*, 2014, **8**, year.
- 22 D. van Noort, S. M. Ong, C. Zhang, S. Zhang, T. Arooz and H. Yu, *Biotechnol Progress*, 2009, **25**, 52–60.
- 23 D. Huh, H. J. Kim, J. P. Fraser, D. E. Shea, M. Khan, A. Bahinski, G. A. Hamilton and D. E. Ingber, *Nat. Protocols*, 2013, **8**, 2135–2157.
- 24 J. H. Sung, M. B. Esch, J.-M. Prot, C. J. Long, A. Smith, J. J. Hickman and M. L. Shuler, *Lab Chip*, 2013, **13**, 1201–1212.
- 25 S. N. Bhatia and D. E. Ingber, *Nat Biotech*, 2014, **32**, 760–772.
- 26 S. J. Trietsch, G. D. Israëls, J. Joore, T. Hankemeier and P. Vulto, *Lab. Chip*, 2013, **13**, 3548–3554.
- 27 P. Vulto, S. Podszun, P. Meyer, C. Hermann, A. Manz and G. A. Urban, *Lab. Chip*, 2011, **11**, 1596–1602.
- 28 E. Yildirim, S. J. Trietsch, J. Joore, A. v. d. Berg, T. Hankemeier and P. Vulto, *Lab Chip*, 2014, **14**, 3334–3340.
- 29 J. Lee, M. J. Cuddihy and N. A. Kotov, *Tissue Engineering Part B: Reviews*, 2008, **14**, 61–86.
- 30 M. W. Tibbitt and K. S. Anseth, *Biotechnol. Bioeng.*, 2009, **103**, 655–663.
- 31 H. K. Kleinman and G. R. Martin, *Semin. Cancer Biol.*, 2005, **15**, 378–386.
- 32 N. Stuurman, A. D. Edelstein, N. Amodaj, K. H. Hoover and R. D. Vale, *Curr Protoc Mol Biol*, 2010.
- 33 J. T. Vogelstein, A. M. Packer, T. A. Machado, T. Sippy, B. Babadi, R. Yuste and L. Paninski, *J Neurophysiol*, 2010, **104**, 3691–3704.
- 34 M. M. Daadi, B. A. Grueter, R. C. Malenka, D. E. Redmond and G. K. Steinberg, *PLoS ONE*, 2012, **7**, e41120.
- 35 Y. Yan, D. Yang, E. D. Zarnowska, Z. Du, B. Werbel, C. Valliere, R. A. Pearce, J. A. Thomson and S.-C. Zhang, *Stem Cells*, 2005, **23**, 781–790.
- 36 P. K. Mattila and P. Lappalainen, *Nat Rev Mol Cell Biol*, 2008, **9**, 446–454.
- 37 S. Iden and J. G. Collard, *Nat Rev Mol Cell Biol*, 2008, **9**, 846–859.
- 38 A. J. Koleske, *Nat Rev Neurosci*, 2013, **14**, 536–550.
- 39 C. Stosiek, O. Garaschuk, K. Holthoff and A. Konnerth, *PNAS*, 2003, **100**, 7319–7324.
- 40 H. C. Johannssen and F. Helmchen, *J Physiol*, 2010, **588**, 3397–3402.
- 41 M. K. Sanghera, M. E. Trulson and D. C. German, *Neuroscience*, 1984, **12**, 793–801.
- 42 W. H. Yung, M. A. Häusser and J. J. Jack, *J Physiol*, 1991, **436**, 643–667.
- 43 P. M. A. Antony, N. J. Diederich, R. Krüger and R. Balling, *FEBS J.*, 2013, **280**, 5981–5993.
- 44 A. A. Grace and B. S. Bunney, *The Journal of neuroscience*, 1984, **4**, 2866–2876.
- 45 P. M. van Midwoud, A. Janse, M. T. Merema, G. M. M. Groothuis and E. Verpoorte, *Anal. Chem.*, 2012, **84**, 3938–3944.
- 46 A. L. Paguirigan and D. J. Beebe, *Integr. Biol.*, 2009, **1**, 182–195.
- 47 M. F. Underhill and C. M. Smales, *Cytotechnology*, 2007, **53**, 47–53.

Captions for Supplementary Movies

Supplementary movie 1: OrganoPlate concept and bioreactor preparation procedure illustrated with a 2-lane bioreactor.

Supplementary movie 2: Three-dimensional distribution of differentiated cells in the culture lane.

Supplementary movie 3: Time lapse of a somatic fluorescences from a spontaneously active TH positive neuron in a 3-lane OrganoPlate, where regular changes in fluorescence are visible. Fluorescence traces were extracted from a manually segmented region of the soma and presented as relative changes in fluorescence ($\Delta F/F$).